1P2-19

Proceedings of Symposium on Ultrasonic Electronics, Vol. 30 (2009) pp. 53-54
18-20 November, 2009

Lateral Detecting Limit of Underground Imaging Owing To Directivity of Sound Source
音源指向特性による地中埋設物映像化の横方向探査範囲

Ryo Toh[1†], Daiki Ando[2] and Seiichi Motooka[1] ([1]Facult. Eng., Chiba Inst. Tech.; [2]Graduate School Eng., Chiba Inst. Tech.)
陶良 [1†]，安藤大樹 [2]，本岡誠一 [1] （[1] 千葉工大 工; [2] 千葉工大 院）

1. Introduction

Efficient technique for imaging objects buried shallowly underground, such as archaeological exploration and pipeline detection, is expected. Though underground radar is popularly used in civil engineering, in an area with many electrolytes or high moisture in the ground, method using ultrasound is considered to be more efficient. In order to acquire images of underground objects with less error images and high resolution, in the condition of field testing with poor original receiving signals influenced by the large attenuation of high-frequency wave and reflection of multiple unevenness in the ground, a three dimensional imaging method using electromagnetic induction (EMI) type sound source and amplitude correlation synthesis processing (ACSP) method was proposed[1-3]. Up to now, the efficiency of the method is verified, and the lateral resolution of the method is studied experimentally.

Considering the directivity of the EMI sound source[4-5] and the nonlinearity of the ACSP signal processing method, this paper discusses of the lateral detecting limit of the method. The relation between the magnitude of images of multiple underground objects with the directivity of the EMI sound source is studied with experiment and numerical simulation. The imaging results of varies arrangement of multiple underground objects show an approxiamate agreement with the theoretical estimation using the directivity of the sound source. And a lateral detecting limit of about 35° spread angle from the sound source can be concluded for this imaging method.

2. EMI sound source

Fig. 1 shows the structure of the EMI sound source, composed of a two layer flat spiral coil cemented on a Bakelite plate, with an aluminum plate placed under it. The electric energy charged in the capacitor is discharged instantaneously to the coil, and the aluminum plate will be driven by the impulsive electromagnetic repulsion force to radiate an intense impulsive sound into the ground.

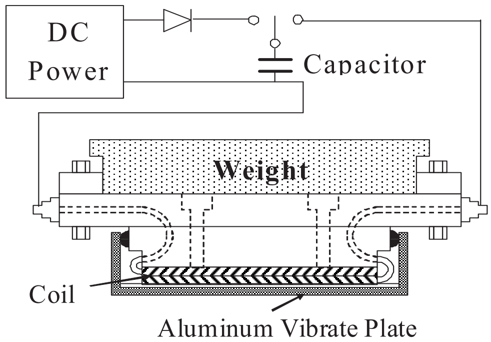

Fig.1 Electromagnetic induction type sound source.

Owing to its particular mechanism, the directivity of radiating sound is different from that of a normal piston vibrating plate, and is given as,

$$R(\theta)=\frac{\mu^2\cos\theta\left(\mu^2-2\sin^2\theta\right)}{\left(2\xi^2-\mu^2\right)^2+4\xi^2\sqrt{\xi^2-1}\sqrt{\xi^2-\mu^2}},\quad(1)$$

where $\xi=\sin\theta$, $\mu^2=\frac{2(1-\sigma)}{1-2\sigma}$, and σ is the Poisson's ratio of the ground.

3. Imaging method

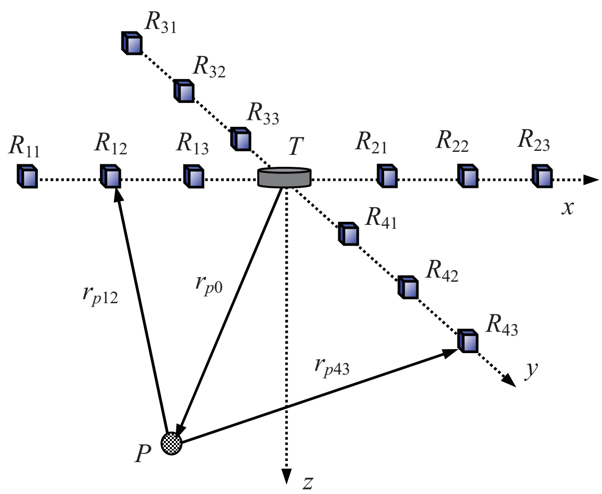

Fig.2 Arrangement of the sound source and receivers.

Fig. 2 shows the arrangement of the sound source and receivers, where the *x-y* plane denotes the ground surface, as well as an underground point *P*. With the sound source *T* as the center of the array, 12 receivers R_{ij}(i=1, 2, 3, 4; j=1, 2, 3) are placed at

---

† liang.tao@it-chiba.ac.jp

an identical interval symmetrically as a cross array.

First, the amplitude and the polarity of each receiving signal at the delay time corresponding to a calculating point P is derived as

$$a_{Pij} = s_{ij}\left(\frac{r_{Pij} + r_{P0}}{c}\right) \quad (i = 1,2,3,4;\ j = 1,2,3)\text{ ,} \tag{2}$$

where c is the sound velocity, and $s_{ij}(t)$ is the signal of receiver R_{ij} preprocessed by normalization with maximum amplitude and compensation by the propagating distance[1]. Then, the 12 signals a_{pij} are divided into 4 groups according to their positions as a_{p1k}, a_{p2l}, a_{p3m}, and a_{p4n} (where $k,\ l,\ m,\ n$=1, 2, 3). Four signals with one from each group are multiplied conditionally as

$$\mathrm{CM}\left(a_{p1k}, a_{p2l}, a_{p3m}, a_{p4n}\right) = \begin{cases} \mathrm{sgn}(a_{p1k}) \cdot \left| a_{p1k} \cdot a_{p2l} \cdot a_{p3m} \cdot a_{p4n} \right|, & \text{4 polarities are same} \\ 0, & \text{otherwise} \end{cases} . \tag{3}$$

$$(k,l,m,n = 1,2,3)$$

Finally, the image magnitude H_p of point P is calculated by synthesizing all the products of conditional multiplication of 81 combinations as

$$H_p = \left| \sum_{k,l,m,n} \mathrm{CM}\left(a_{p1k}, a_{p2l}, a_{p3m}, a_{p4n}\right) \right| . \tag{4}$$

4. Experimental conditions and results

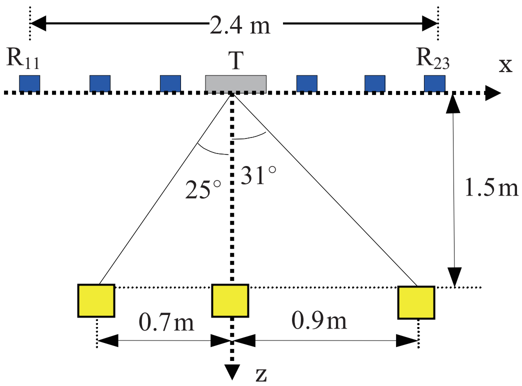

a) Testing position.

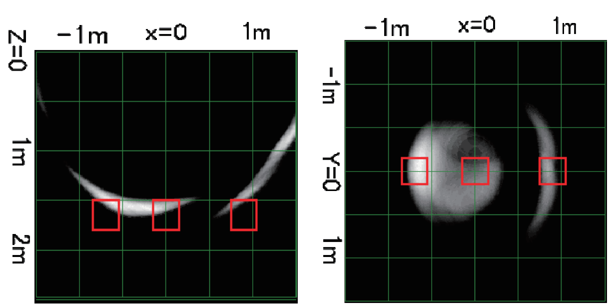

b) Vertical projection. c) Horizontal projection.

Fig.3 Example imaging result.

Fig. 3 shows an example of the testing position together with the imaging results. Three concrete blocks (0.3m × 0.3m × 0.3m) are buried in a horizontal line along the x-axis (y=0) in an experimental sand field with intervals of 0.7m and 0.9m. By moving the sound source and receiver array and digging down the ground surface, three positions with two buried depth are measured.

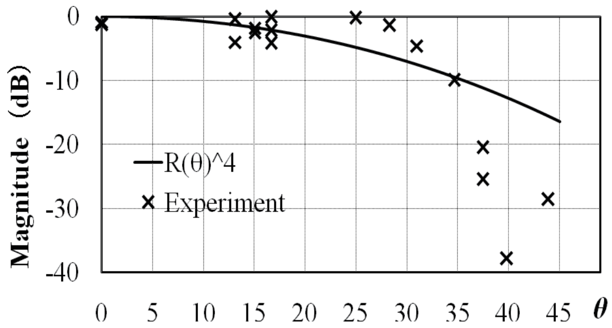

Fig.4 Distribution of imaging magnitudes with spread angle from EMI sound source.

Fig. 4 shows the magnitudes around the buried objects in the imaging results versus the spread angle from the central axis of EMI sound source according to their positions. In order to discuss the tendency of the magnitude of image with the spread angle, all the results of six measurements are shown together. Here, because of the considerable distortion of image from its corresponding buried position, the maximum magnitudes in a 0.3m × 0.3m × 0.3m range with the center of buried positions are picked out as imaging magnitude data. Moreover, as a theoretical estimation, the magnitude calculated by $R(\theta)^4$ is also shown. The fourth power of directivity of the sound source is calculated owing to the nonlinear processing that multiplies four reflected signals.

It is shown in Fig. 4 that the distribution of imaging magnitude according to different spread angle agrees approximately with the simple theoretical estimation. The radical decrease of image magnitudes at larger angle can be explained that the ACSP calculates the magnitude with an additional polarity condition. Also, it shows a same result with the underground images not presented here that the buried objects at positions with spread angle of sound source larger than 35° can hardly to be imaged, within the dynamic range of -20 dB.

Acknowledgment

This work was partially supported by JSPS through Grant-in-Aid for scientific research.

References

1. Y. Matsuo, L. Tao and S. Motooka: Jpn. J. Appl. Phys. **41** (2002) 3539.
2. L. Tao, T. Watanabe and S. Motooka: Nihon Onkyo Gakkaishi. **60** (2004) 727.[in Japanese]
3. L. Tao and S. Motooka: Jpn. J. Appl. Phys. **46** (2007) 4589.
4. S. Motooka and L. Tao: Nihon Onkyo Gakkaishi. **58** (2002) 611. [in Japanese]